NEW ZEALAND SOCIETY FOR EARTHQUAKE ENGINEERING
2019 Pacific Conference on Earthquake Engineering
TURNING HAZARD AWARENESS INTO RISK MITIGATION
4 – 6 April | SkyCity, Auckland | New Zealand

Undrained monotonic behaviour of liquefied pumiceous sands

M.S. Asadi, R.P. Orense, M.B. Asadi & M.J. Pender
Department of Civil & Environmental Engineering, University of Auckland, Auckland, New Zealand.

ABSTRACT

There have been questions as to whether the post-liquefaction stress-strain behaviour of crushable pumice sands is similar to those of hard-grained sands. In order to shed light on this, several series of advanced element tests using a cyclic triaxial apparatus were conducted on different natural pumice (NP) sands sourced from the Waikato Region and on hard-grained Toyoura sand to investigate the effect of relative density on their post-liquefaction response. The sand specimens, reconstituted at different relative densities, were tested under various levels of cyclic stress ratio. When the onset of liquefaction was monitored, the cyclic load was stopped after which monotonic load was applied under undrained condition to obtain the stress-strain relation of the liquefied sand. The post-liquefaction behaviour was modelled in the form of bi-linear stress-strain curve, which was characterised by three parameters: the initial modulus (E_1), the modulus at recovery (E_2); and the recovery strain ($\mathcal{E}_r$), corresponding to the level when the sand started to recover its strength. The results illustrated that NP sands showed significantly different post-liquefaction behaviour when compared to Toyoura sand. NP sands have much higher E_1 due, partly at least, to the high angularity of the pumice particles which induced particle interlocking when sheared. NP sands required smaller $\mathcal{E}_r$ to mobilise strength recovery which, owing to their more dilative response, resulted in early decrease in excess pore water pressure. However, during the recovery phase, E_2 of NP sands was much lower, partially due to the occurrence of particle crushing.

1 INTRODUCTION

The post-liquefaction behaviour of sand is important because following an earthquake, the liquefied sand would be in a transient state of almost zero effective stress and the application of shear stress would cause the sand to undergo large deformation with almost zero strength. Such deformation of the ground can cause severe damage to infrastructure, including embankments and dams. The deformation of sand following liquefaction is affected by many factors, including sand type and relative density. Although many researchers

have investigated and clarified the post-liquefaction behaviour of hard-grained sandy materials in the laboratory using post-cyclic monotonic undrained tests (e.g. Yasuda et al. 1995; Sitharam et al. 2009; Rouholamin et al. 2017), little is known about the post-liquefaction response of natural pumice sands, i.e. mixture of pumice particles with other hard-grained constituents.

Crushable volcanic sands are found in several areas in the central part of the North Island, mainly as a result of volcanic eruptions centred in the Taupo Volcanic Zone (TVZ). The pumice-rich pyroclastic flows from these eruptions were transported airborne and then deposited in wide areas through erosion and river transport in the Waikato Basin. In the process, the pumice particles were mixed with other soils in the area, and the deposits are herein referred to as natural pumice (NP) sands. Pumice particles are characterised by their crushability and compressibility, and recent studies indicate that their cyclic and liquefaction behaviour are different from those of quartz-based hard-grained sands (Orense et al. 2012; Orense & Pender 2015; Asadi et al. 2018).

This paper investigates the post-liquefaction monotonic response of reconstituted NP sands prepared at different relative densities. For comparison purposes, similar tests were also performed on Toyoura sand, a hard-grained sand.

2 MATERIALS USED AND TESTING PROGRAMME

Disturbed NP sands were obtained as bulk samples from test pits at sites NP1, NP2 and NP3 within the Waikato Basin. Figure 1(a) shows the location of the sites. Sites NP1 and NP2 were located in Hamilton City while site NP3 was near Rangiriri Town. The NP materials were sourced at depths of 1.5 m, 2.0 m and 4.5 m, respectively, for NP1, NP2 and NP3 sites. These depths were chosen because borehole logs showed the presence of pumice-rich layers. For comparison purposes, Toyoura sand, a well-known hard-grained, sub-angular material, was also used to perform the laboratory tests. The index properties of the materials tested are summarised in Table 1 while the particle size distribution (PSD) curves are shown in Figure 1(b).

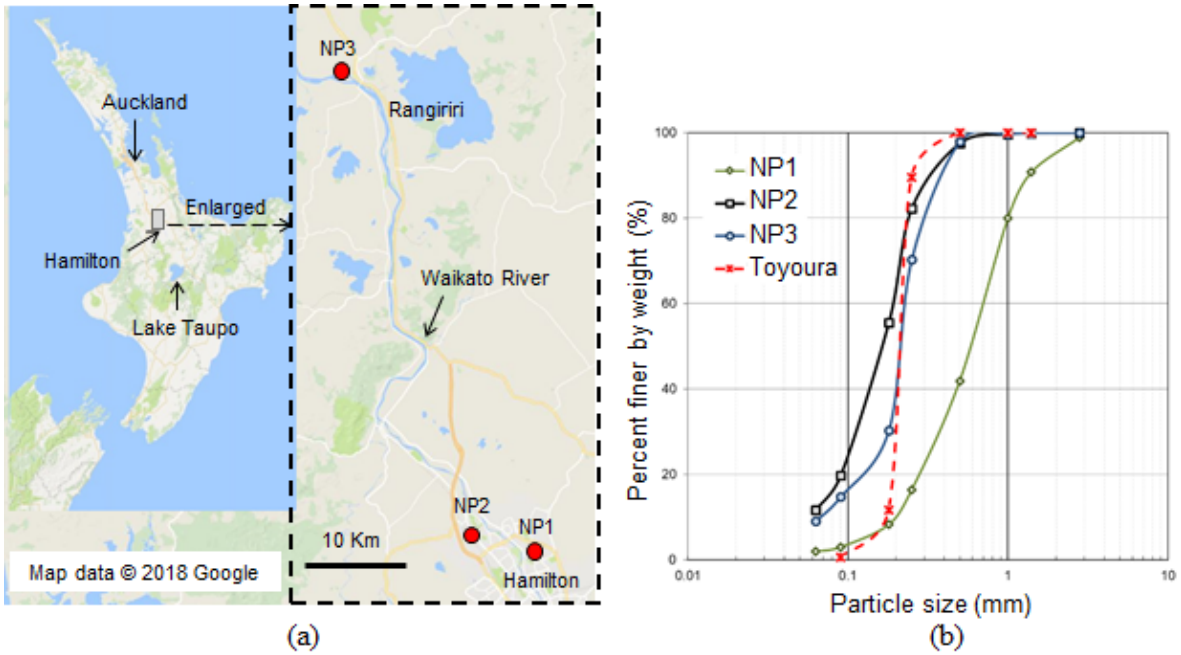

Figure 1: (a) Locations where the natural pumiceous materials were sampled (map data © 2018 Google); and (b) particle size distribution curves of the materials tested.

The specimens, with target size of 63 mm diameter and 126 mm height, were prepared by moist tamping method with target relative density after consolidation corresponding to loose (D_r = 30%), medium-dense (D_r

Table 1: Index properties of the materials tested

Material	Specific gravity	Maximum dry density (g/cm^3)	Minimum dry density (g/cm^3)
NP1	2.53	1.54	1.27
NP2	2.50	1.38	1.07
NP3	2.54	1.24	0.93
Toyoura sand	2.66	1.64	1.40

= 50%) and dense (D_r = 80%) conditions. The specimens were fully saturated by gradually increasing the cell and back pressures over a period of 24 hours. Once subsequent check showed B-value in excess of 0.95, the specimen was isotropically consolidated under an effective confining pressure σ'_c = 100 kPa. Then, the specimen was made to liquefy by applying a specified level of cyclic stress ratio (*CSR*) with frequency of 0.1 Hz under undrained conditions.

Once the specimen liquefied (i.e. when double amplitude axial strain of $\mathcal{E}_{DA}$= 5% was reached), the cyclic loading was terminated and the specimen was subjected to undrained monotonic loading at a rate of 0.01 mm/sec without allowing the excess pore water pressure (*EPWP*) to dissipate. Since it was difficult to stop all tests at exactly the same state, attempts were made to stop the cyclic loading on the extension side, where the specimens were in a transient state with almost zero effective stress. Thus, with the application of shear stress, the specimens underwent some deformation with almost zero strength. For the purpose of the analysis, the initial height (h_i) of the specimen before cyclic loading was used as reference, i.e. zero (0%) axial strain corresponded to the initial height of specimen; a negative axial strain as starting point indicated that the post-cyclic monotonic loading started when the specimen was in the extension condition. It was observed that during monotonic loading, the specimen had the tendency to follow the same stress-strain relation as the last cyclic loading path, indicating that it remembered the last loading history it experienced.

To characterise the behaviour of the liquefied sand, the stress–strain curve of the sand was divided into three distinct regions (Thomas 1992; Thomas & Vaid 1995): (1) Region 1, characterised by essentially zero stiffness (the stiffness of the sand is almost zero and the specimen would undergo extensive deformation until it recovers its stiffness); (2) Region 2, where stiffness continually increases (coincides with a parabolic curve, indicating the sand stiffness increases with straining); and (3) Region 3 where the stiffness is essentially constant (i.e. the linear part of the stress–strain curve where the shear modulus is constant).

In examining the post–liquefaction behaviour of the tested materials, the following parameters were used, as illustrated in Figure 2: (1) Initial modulus, E_1: the minimum slope of the stress-strain curve in Region 1; (2) Recovery strain, $\mathcal{E}_r$: the strain where the strength of the liquefied specimen suddenly increases (i.e. axial strain required to mobilize 1 kPa of axial stress) and corresponds to the start of Region 2; and (3) Modulus at recovery, E_2: the maximum slope of the linear part of the stress–strain curve corresponding to Region 3.

3 TEST RESULTS

3.1 Response of liquefied sands

Post-liquefaction monotonic tests were performed on reconstituted specimens with different relative densities, D_r; typical post-liquefaction undrained monotonic behaviour of NP2 sand, as a representative of the NP materials tested, is shown in Figure 3 for the D_r = 30%, 50% and 80% conditions under the same σ'_c

= 100 kPa. The data depicted in the figures are the results for those specimens that liquefied ($\mathcal{E}_{DA}$= 5%) after essentially similar number of cycles (indicated in each figure, together with the applied *CSR*).

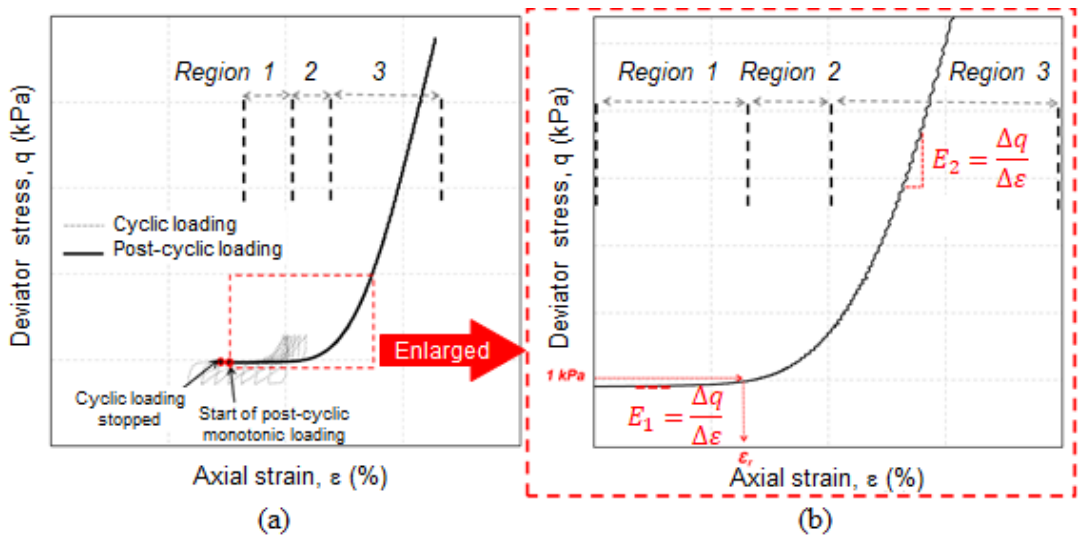

Figure 2: (a) Schematic of post-cyclic behaviour of liquefied sand; (b) enlarged view of indicated section.

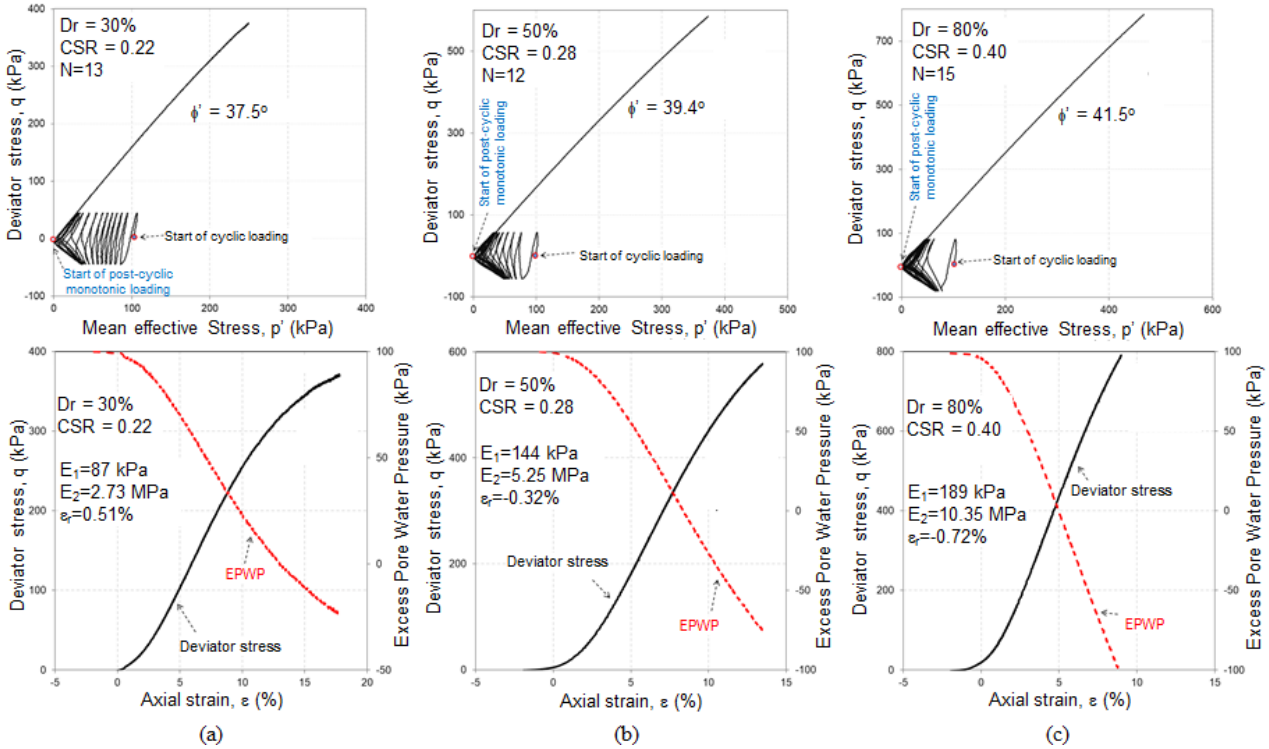

Figure 3: Typical post-liquefaction response of NP2 sand in terms of effective stress path (upper plot) and development of deviator stress and excess pore water pressure with axial strain (lower plot) for: (a) loose (D_r ≈ 30%); (b) medium dense (D_r ≈ 50%); and (c) dense (D_r ≈ 80%) conditions.

The following can be seen from the figure: (1) during cyclic loading the specimens showed contractive behaviour, and the mean effective stress decreased gradually from the initial value towards zero; the state of almost zero mean effective stress was observed for all specimens regardless of relative density; (2) the NP2 sand, regardless of its relative density, always showed strain-hardening behaviour during post-cyclic shearing; (3) the inter-particle friction angle (ϕ) of dense NP2 material with D_r = 80% (41.5°) is significantly higher than that of NP2 sand in loose condition (37.5°) and in medium-dense condition (39.4˚); and (4) the

liquefied specimens underwent some deformation with almost zero stiffness, irrespective of their initial relative density. However, some differences in the responses of loose and dense specimens were also observed and these will be discussed later.

To examine the influence of initial relative density on the stress–strain behaviour of liquefied NP sands, the results of the post-liquefaction monotonic tests on NP1, NP2 and NP3 sands with relative densities of 30%, 50% and 80% are shown in Figure 4. As expected, relative density played an important role in the post-liquefaction behaviour of NP sands: (1) the length of Region 1 decreased with increasing relative density, resulting in $\mathcal{E}_r$ of loose specimens being greater than that of dense specimens; (2) the strength recovery of dense NP specimens occurs at considerably lower strain than that of loose specimens, causing Region 2 for dense specimens to be smaller; and (3) the E_1 and E_2 of NP sands increase with increasing relative density, with dense specimens showing stiffer response at Region 3 than medium-dense and loose specimens.

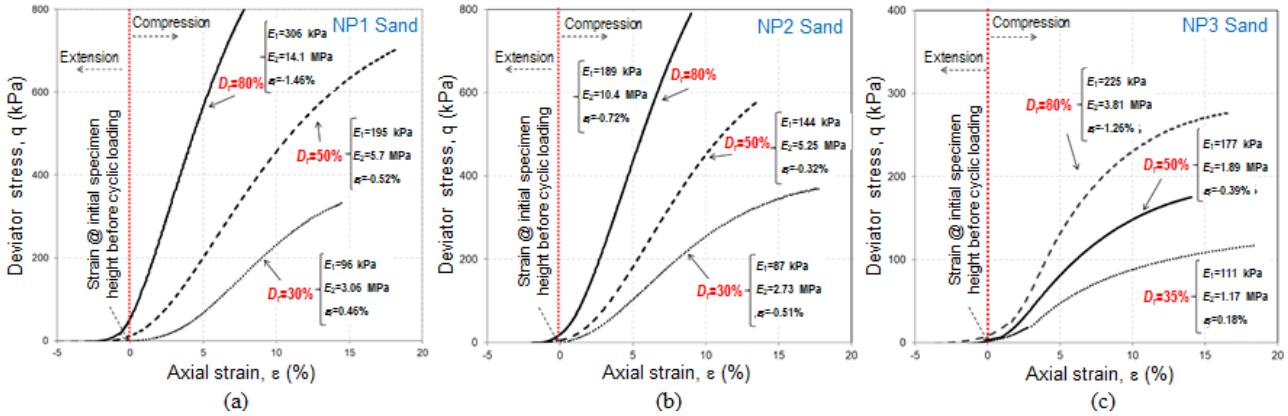

Figure 4: Effect of relative density on the stress-strain curves of liquefied (a) NP1; (b) NP2; and (c) NP3 sands.

The different responses of loose, medium-dense and dense liquefied NP sands can be attributed to the voids between the particles being minimal in the dense condition; i.e., at dense condition, there are less voids in the specimen and following liquefaction (cyclic mobility), the sand grains immediately come in contact with each other during post-liquefaction loading, resulting in immediate recovery of their strength (dilative response). In loose condition, there are more voids between particles and consequently more deformation is required for strength to recover or for the particles to come into contact. Note that the different levels of *CSR* applied to the specimens during cyclic loading may also have some effects on the undrained behaviour of the liquefied specimens; however, these are beyond the scope of the present study.

3.2 Particle crushing investigation

As reported by Asadi et al. (2018), NP sands underwent some particle crushing during cyclic loading. To investigate the occurrence of particle crushing during post-liquefaction monotonic loading, the multi-stage triaxial tests conducted under the same initial conditions (the same relative density, confining pressure and *CSR*) were terminated at different stages: (1) at the end of cyclic loading; and (2) at the end of post-liquefaction monotonic loading. Sieve tests were then performed to determine the PSD of the samples, and the results for NP2 sands are depicted in Figure 5(a). Next, the method of Hardin (1985) was used to quantify the particle crushing of NP sands during post-cyclic testing. In this method, the area enclosed by the PSD curves before and after the tests and the line corresponding to 0.063 mm was used to calculate the total breakage B_t. The relative breakage ($B_r = B_t/B_{po}$, where the initial potential breakage (B_{po}) is the enclosed area between the PSD curves before the tests and the line corresponding to 0.063 mm) was used to make comparison of results on samples with different PSD easier. The relationship between relative breakage and relative density at the end of both cyclic loading and post-liquefaction monotonic loading is shown in Figure

5(b). All NP sands underwent some particle crushing during both cyclic and post-cyclic testing. Based on the limited number of tests, it appeared that the relative breakage during cyclic loading for all NP sands is higher than that during post-liquefaction monotonic loading and the NP sands experienced different levels of particle crushing; i.e. the NP3 sand has higher relative breakage than NP2 sand while NP1 sand experienced the least relative breakage. This may be due to the amount of pumice content in the NP sands; however quantification of pumice content is beyond the scope of this paper.

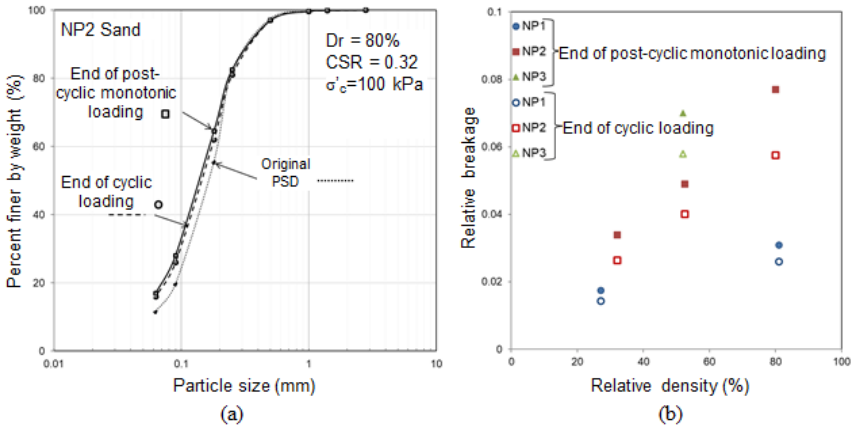

Figure 5: (a) Typical particle size distribution curves of NP2 sand at different stages of the multi-stage triaxial testing; and (b) comparison of the relative breakage of the materials at the end of cyclic testing and at the end of post-cyclic monotonic testing.

3.3 Comparison of NP sands and Toyoura sand

The post-liquefaction responses of NP2 sands were compared with Toyoura sand to investigate the influence of particle characteristics on the post-liquefaction response. Figures 6 show typical post-liquefaction undrained monotonic behaviour of Toyoura sand and NP2 sand (as a representative of NP sands). Furthermore, the E_1, E_2 and $\mathcal{E}_r$ of NP1, NP2, NP3 and Toyoura sands for different relative densities are compared in Figure 7. The following observations can be made from the figures:

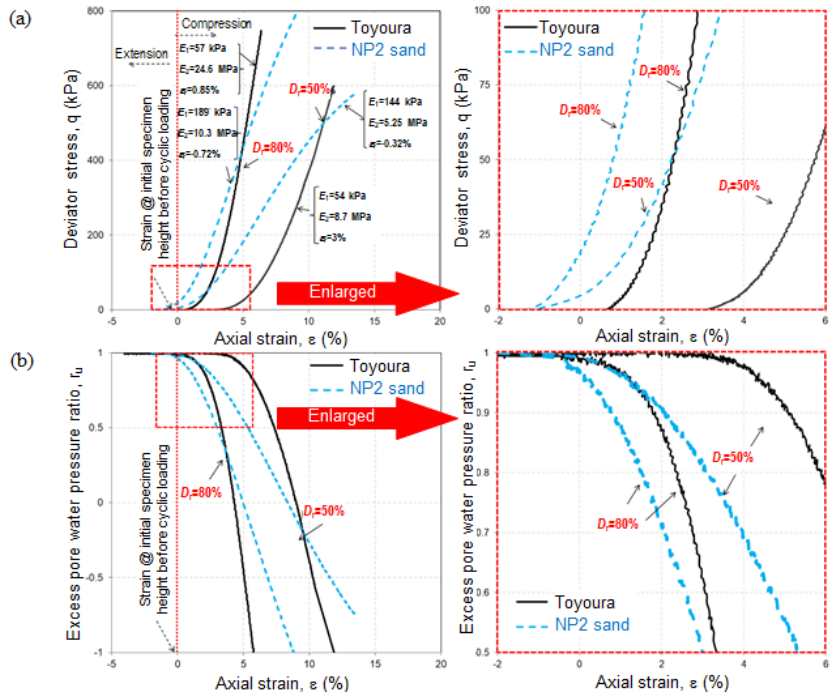

Figure 6: (a) Stress-strain curves; and (b) excess pore water pressure responses of Toyoura and NP2 sands. The plots on the right are the enlarged views of the sections indicated in the left plots.

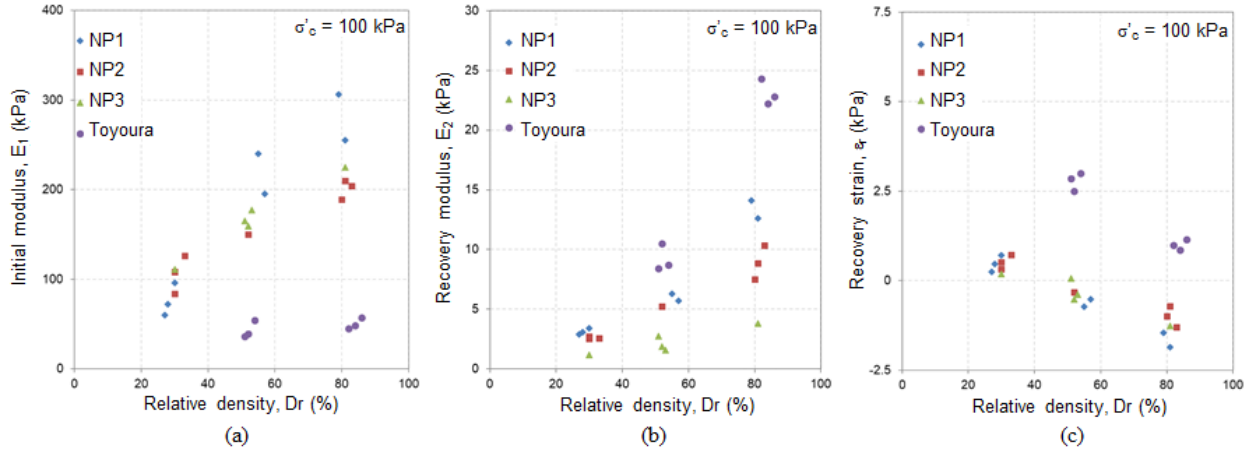

Figure 7: Relation between: (a) initial modulus, E_1; (b) recovery modulus, E_2; and (c) recovery strain ($\mathcal{E}_r$) and relative density, D_r, for NP sands and Toyoura sand.

(1) The strength recovery of liquefied Toyoura sand was more affected by relative density than that of pumiceous sand. For instance, medium-dense Toyoura sand underwent more deformation with almost zero strength compared with the dense condition. The recovery strain of medium-dense Toyoura sand ($\mathcal{E}_r$ = 3.0%) was higher than that of dense specimens ($\mathcal{E}_r$ = 0.85%); on the other hand, the recovery strains of medium-dense and dense NP2 sand was approximately the same ($\mathcal{E}_r$ = -0.72% to -0.32%).

(2) The excess pore water pressure ratio ($r_u = EPWP/\sigma'_c$) of Toyoura and NP2 sands decreased as a result of post-liquefaction monotonic loading. In Regions 1 and 2, the rate of decrease in r_u of NP2 sand was faster than that of Toyoura sand, while in Region 3, (under further loading and more straining) the rate of decrease in r_u of Toyoura sand became faster.

(3) The E_1 of NP sands was higher than that of Toyoura sand); for example, E_1 of dense Toyoura sand is 57 kPa while that of dense NP2 sand is 189 kPa. In contrast, E_2 of Toyoura sand was considerably higher than those of NP sands with similar relative density; for instance, E_2 of dense Toyoura sand (24.6 MPa) was almost 2.3 times higher than that of dense NP2 sand (10.35 MPa).

(4) The length of Region 1 for NP sands was considerably shorter than that of Toyoura sand (for the same relative density), indicating that during post-cyclic monotonic loading, the NP sands recovered their stiffness at a considerably lower strain level than Toyoura sand. For instance, at medium-dense relative density of 50%, Toyoura sand underwent more than 3% axial strain with almost zero strength; however, NP2 sand with the same relative density recovered its stiffness at a significantly smaller strain level (around -0.32%) and at 0% strain corresponding to the initial height of the specimen before cyclic loading, NP2 sand had some stiffness.

The different behaviour of liquefied Toyoura and NP sands under monotonic loading can be attributed to different changes in fabric within the specimens during cyclic loading and to the occurrence of particle crushing during cyclic and post-liquefaction testing. It is hypothesized that at Regions 1 and 2, due to the low level of stress applied, the amount of particle crushing is negligible and thus the angularity of the pumice particle components plays a dominant role. At Region 3, however, the increased level of stress causes small amount of particle crushing to occur, which has an important influence on the response of NP sands. As reported by Asadi et al. (2018), particle crushing of NP sands during cyclic loading and the angularity of the pumice particles lead to the formation of a stable sand skeleton inside the specimen, due to interlocking between particles during shearing. Hence, NP sands recover their stiffness earlier (the recovery strain of the NP sand is smaller than that of Toyoura sand) and the E_1 of the NP sand is higher than that of Toyoura sand. However, because of particle crushing at Region 3, the E_2 of the NP sand is smaller than that of Toyoura sand and the rate of decrease in EPWP of Toyoura sand also becomes faster compared to NP sands. Note that

the responses obtained for Toyoura sand were consistent with those reported in the literature for other hard-grained sands (e.g. Rouholamin et al., 2017).

4 CONCLUSIONS

To investigate the post-liquefaction monotonic response of reconstituted natural pumiceous (NP) sands and Toyoura sand, liquefied specimens were subjected to monotonic loading without allowing the excess pore water pressure to dissipate. The following conclusions can be drawn from the test results:

- During post-liquefaction monotonic loading, a strain-hardening response was observed for both NP and Toyoura sands regardless of the initial relative density.
- Relative density played an important role in the post-liquefaction response of NP sands; as the relative density increased, the specimens started to recover their strength more quickly (i.e. at a lower recovery strain, $\mathcal{E}_r$).
- The effect of relative density on the recovery strain of the NP sands was less pronounced than that for Toyoura sand; for instance the recovery strains of medium-dense and dense NP2 sands were almost the same which was in contrast to the observed behaviour of Toyoura sand.
- The post-liquefaction monotonic response of NP sand was different from that of Toyoura sand. Due to their irregular surface texture, the liquefied NP sands recovered their strength at a considerably smaller strain level and had higher initial Young's modulus (E_1) values compared with Toyoura sand. However, due to particle crushing during the post-cyclic testing, the NP sands had lower values of modulus at recovery (E_2) compared with Toyoura sand.

ACKNOWLEDGMENT

The assistance of geotechnical engineers from Opus International Consultants Ltd. in facilitating access to the sites and in providing some samples and site details is gratefully acknowledged. The authors would also like to thank Jeff Melster, Lu Yi, Yuan Hong and Mark Liew of the University of Auckland for the assistance provided during sampling.

REFERENCES

Asadi, M.S., Asadi, M.B., Orense, R.P. & Pender, M.J. 2018. Undrained cyclic behavior of reconstituted natural pumiceous sands. *Journal of Geotechnical and Geoenvironmental Engineering, ASCE*, 144 (8), 04018045.

Hardin, B.O. 1985. Crushing of soil particles. *Journal of Geotechnical Engineering, ASCE*, 111 (10), 1177-1192.

Orense, R.P., Pender, M.J. & O'Sullivan, A. 2012. Liquefaction characteristics of pumice sands. *Report No. EQC 10/589*. University of Auckland.

Orense, R.P. & Pender, M.J. 2015. From micro to macro: An investigation of the geomechanical behaviour of pumice sand, *Keynote Lecture, International Workshop on Volcanic Rocks & Soils*, Isles of Ischia, Italy, 45-62.

Rouholamin, M., Bhattacharya, S., & Orense, R.P. 2017. Effect of initial relative density on the post-liquefaction behaviour of sand. *Soil Dynamics and Earthquake Engineering*, 97, 25-36.

Sitharam, T.G., Vinod, J.S. & Ravishankar, B.V. 2009. Post-liquefaction undrained monotonic behaviour of sands: Experiments and DEM simulations. *Geotechnique*, 59 (9), 739-749.

Thomas, J. 1992. Static, cyclic and post liquefaction undrained behaviour of Fraser river sand. *PhD Thesis*, University of British Columbia.

Vaid, Y.P. & Thomas, J. 1995. Liquefaction and post-liquefaction behavior of sand. *Journal of Geotechnical Engineering, ASCE*, 121 (2), 163-173.

Yasuda, S., Yoshida, N., Masuda, T., Nagase, H., Mine, K. & Kiku, H. 1995. Stress-strain relationships of liquefied sands. *International Conference on Recent Advances in Geotechnical Earthquake Engineering and Soil Dynamics*, St. Louis, Missouri, 295-298.